

# UCLA

## UCLA Previously Published Works

### Title

Cofilin-induced changes in F-actin detected via cross-linking with benzophenone-4-maleimide.

### Permalink

<https://escholarship.org/uc/item/9b10d0s8>

### Journal

Biochemistry, 52(32)

### Authors

Chen, Christine

Benchaar, Sabrina

Phan, Mai

et al.

### Publication Date

2013-08-13

### DOI

10.1021/bi400715z

Peer reviewed

Published in final edited form as:

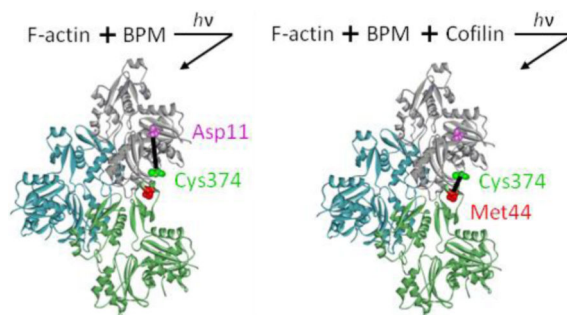
Biochemistry. 2013 August 13; 52(32): 5503–5509. doi:10.1021/bi400715z.

## Cofilin-Induced Changes in F-Actin Detected via Cross-Linking with Benzophenone-4-maleimide

Christine K. Chen, Sabrina A. Benchaar, Mai Phan, Elena E. Grintsevich, Rachel R. Ogorzalek Loo, Joseph A. Loo, and Emil Reisler\*

Department of Chemistry and Biochemistry, Molecular Biology Institute and Biological Chemistry, University of California, Los Angeles, Los Angeles, California 90095, United States

### Abstract



Cofilin is a member of the actin depolymerizing factor (ADF)/cofilin family of proteins. It plays a key role in actin dynamics by promoting disassembly and assembly of actin filaments. Upon its binding, cofilin has been shown to bridge two adjacent protomers in filamentous actin (F-actin) and promote the displacement and disordering of subdomain 2 of actin. Here, we present evidence for cofilin promoting a new structural change in the actin filament, as detected via a switch in cross-linking sites. Benzophenone-4-maleimide, which normally forms intramolecular cross-linking in F-actin, cross-links F-actin intermolecularly upon cofilin binding. We mapped the cross-linking sites and found that in the absence of cofilin intramolecular cross-linking occurred between residues Cys374 and Asp11. In contrast, cofilin shifts the cross-linking by this reagent to intermolecular, between residue Cys374, located within subdomain 1 of the upper protomer, and Met44, located in subdomain 2 of the lower protomer. The intermolecular cross-linking of F-actin slows the rate of cofilin dissociation from the filaments and decreases the effect of ionic strength on cofilin–actin binding. These results are consistent with a significant role of filament flexibility in cofilin–actin interactions.

Rapid remodeling of the actin cytoskeleton is essential for many cellular processes in eukaryotic organisms including cell motility, differentiation, and division. Proteins belonging to the actin-depolymerizing factor (ADF)/cofilin family play a key role in regulating actin dynamics.<sup>1</sup> As the name implies, ADF/ cofilin is able to enhance actin

treadmilling by binding to ADP-actin with high affinity and promoting disassembly of actin filaments (F-actin) from the pointed end. Cofilin binds to F-actin, promoting its severing and thus creating more ends for depolymerization or polymerization.<sup>2,3</sup> Because cofilin plays a complex role in actin dynamics and is a ubiquitous protein, it is important to obtain the best possible structural characterization of cofilin's interaction with F-actin.

Prior to the most recent ~9 Å resolution model of cofilin bound to F-actin,<sup>4</sup> several groups have mapped the binding sites of cofilin on both G- and F-actin via mutagenesis, fluorescence probing, and chemical cross-linking in an effort to understand cofilin's functions.<sup>5–9</sup> Grintsevich et al.<sup>5</sup> concluded that cofilin binds to the hydrophobic cleft between subdomains 1 and 3 on G-actin, as suggested by previous models.<sup>10,11</sup> The atomic structure of the C-terminal ADF homology domain of twinfilin in complex with G-actin also supports binding between subdomains 1 and 3 of G-actin. The ADF homology domain inserts an  $\alpha$ -helix into the hydrophobic cleft on actin in a similar manner to gelsolin and WH2 domain proteins.<sup>12</sup> The structure of cofilin–G-actin provides insight into the mechanism for ADF depolymerization of actin through the weakening of intrafilament interactions. Electron microscopy (EM) reconstructions, chemical cross-linking, and molecular dynamic (MD) simulations also lead to a model of the cofilin/ F-actin complex.<sup>10,13–16</sup> Galkin et al.<sup>4</sup> showed that cofilin binding displaces substantially the subdomain 2 of actin and results in its disordering, thus disrupting interprotomer contacts. The disordering of subdomain 2 caused by cofilin binding leads to a 4-fold increase in F-actin flexibility.<sup>17</sup> As for filament stability, the impact of disrupting interprotomer contacts is offset to a great extent by cofilin's binding to two adjacent longitudinal actin protomers.

Here, we provide experimental evidence derived from actin cross-linking by benzophenone-4-maleimide (BPM) for two types of structural transitions in actin: one associated with actin polymerization into filaments and the other coupled to cofilin binding to F-actin. Although cross-linking captures changes that normally reflect contact-induced modification of specific sites, it is believed that actin polymerization prompts intramolecular changes as well.

Previous results from Tao et al.<sup>18</sup> showed little or no cross-linking in G-actin after Cys374 labeling with BPM. However, intramolecular BPM cross-linking was detected after G-actin polymerization into F-actin. We confirm here this observation and map the intramolecular cross-link in F-actin to Cys374 and Asp11. Binding of cofilin to F-actin replaces this intramolecular cross-link with an intermolecular cross-link from Cys374 to Met44. We also report differences in dissociation of cofilin from cross-linked and un-cross-linked F-actin indicative of the need for filament flexibility in cofilin dissociation. Cofilin-induced conformational changes may help elucidate the local and global changes that occur in F-actin and destabilize certain interprotomer contacts.

## MATERIALS AND METHODS

### Materials

Benzophenone-4-maleimide and acrylodan were obtained from Molecular Probes (Eugene, OR). *N*-(4-Azido-2-nitrophenyl)putrescine (ANP) was synthesized as described.<sup>19</sup> Milli-Q-filtered water (Millipore) and analytical grade reagents were used in all experiments.

### Protein Purification and Labeling

Actin was purified from acetone powder of rabbit skeletal muscle as described previously.<sup>20</sup> Recombinant *S. cerevisiae* wild type cofilin and cofilin-Cys1 mutant (C1/C62S) in pBAT4 vector were expressed and purified as described<sup>5</sup> with slight modifications. Cys1 on cofilin mutant was labeled with acrylodan by first passing the protein through a Zeba Desalt Spin Column (Pierce) equilibrated with 10 mM Tris pH 8.0. Cofilin was labeled at 1 mg/mL with a 3 times molar excess of acrylodan and incubated on ice for 2 h. The reaction was stopped with 1 mM DTT, and the protein was dialyzed overnight in 5 mM Hepes pH 7.5 and 1 mM DTT to remove excess label. Labeling efficiency was characterized by using an adjusted extinction coefficient (determined as before,<sup>21</sup> with slight modifications). The absorbance of acrylodan was measured first in methanol ( $\epsilon = 20\,000\text{ M}^{-1}\text{ cm}^{-1}$ ,  $\lambda_{\text{max}} = 391\text{ nm}$ ) (Molecular Probes, The Handbook) and then under denaturing conditions, with 6 M guanidine-HCl ( $\lambda_{\text{max}} = 411\text{ nm}$ ). The absorbance ratio [ $A_{\text{max}}(\text{methanol})/A_{\text{max}}(\text{Gu-HCl}) = 1.5$ ] was used to correct the extinction coefficient determined in methanol for denaturing conditions ( $20\,000\text{ M}^{-1}\text{ cm}^{-1}/1.5 = 13\,333\text{ M}^{-1}\text{ cm}^{-1}$ ). Cofilin mutant concentration was measured by the Bradford assay using wild-type cofilin as a standard.

### ANP and BPM Cross-Linking

ANP cross-linking was performed as described previously.<sup>22</sup> BPM cross-linking was executed as described previously<sup>18</sup> with a few modifications. DTT was removed from G-actin on a PD-10 column (GE Healthcare) equilibrated with G-buffer (5 mM Tris pH 8.0, 0.2 mM CaCl<sub>2</sub>, 0.4 mM ATP). BPM and actin (at 2:1 molar ratio) were incubated overnight at 4 °C. Labeled G-actin was passed through a PD-10 column equilibrated with G-buffer (5 mM Hepes pH 7.5, 0.2 mM CaCl<sub>2</sub>, 0.2 mM ATP) to remove excess label. Labeled actin was polymerized with 2 mM MgCl<sub>2</sub> and 50 mM KCl for 30 min at room temperature. Cofilin-Cys1 mutant was passed through Zeba Desalt Spin Columns equilibrated with G-buffer. Labeled actin was incubated with and without DTT-free cofilin and cross-linked under UV light (365 nm) for up to 90 min. The reaction was stopped with DTT.

### Electron Microscopy

BPM-F-actin was cross-linked in the presence of cofilin at a 1:3 mole ratio to actin. Cross-linked F-actin was incubated with 1.0 M KCl for 20 min and then pelleted in an OPTIMA-TLX120 ultracentrifuge (Beckman Coulters) at 350000g for 20 min. Cross-linked F-actin was depolymerized by dialysis vs G-actin buffer. BPM-cross-linked dimers were further purified on a SuperdexS200 16/60 cm gel filtration column (GE Healthcare).

For actin filament visualization, all samples were diluted to 2  $\mu\text{M}$  in F-buffer (10 mM Tris pH 8.0, 2 mM MgCl<sub>2</sub>, 100 mM KCl, 0.2 mM ATP) and deposited on 400-mesh carbon-

coated copper grids coated with Formvar film (Ted Pella Inc., Redding, CA). Samples were allowed to adsorb for 60 s and then negatively stained with 1% uranyl acetate (w/v) for 45 s. Grids were observed with a JEM-1200EX (JEOL) electron microscope operated at 80 kV and magnification in the 80000–100000 $\times$  range. The images were analyzed using ImageJ software.

### Mass Spectrometry

Cross-linked F-actin was depolymerized in G-buffer (pH 8.0). An equimolar amount of Kabiramide C was added to actin prior to its purification on a SuperdexS200 16/60 cm gel filtration column (GE Healthcare).

Cross-linked actin (1 mg/mL) was reduced with 10 mM DTT at 60 °C for 45 min and alkylated with 24 mM iodoacetamide at 45 °C for 1 h. Cross-linked actin was digested with Lys-C and then with trypsin at a 1:50 enzyme:substrate ratio in 300 mM Tris-HCl (pH 8.0). The first digest was incubated at 37 °C for 24 h and then for another 24 h after addition of trypsin. Online peptide sequencing was accomplished by liquid chromatography–tandem mass spectrometry (LC-MS/MS) with a QSTAR XL quadrupole time-of-flight (QqTOF) mass spectrometer (Applied Biosystems, Foster City, CA). The nano-LC was equipped with an LC Packings PepMap C18 precolumn (300  $\mu$ m  $\times$  5 mm) and an LC Packings PepMap analytical reversed-phase C18 column (75  $\mu$ m  $\times$  150 mm). The eluents used for the LC were (A) 5% acetonitrile (ACN)/water containing 0.1% formic acid (FA) and 0.01% trifluoroacetic acid (TFA) and (B) 95% ACN/water acid containing 0.1% FA and 0.01% TFA. The flow rate was 200 nL/min, and the following gradient was used: 5% B to 35% B in 15 min, then 35% B to 80% B in 4 min, and then maintained at 80% B for 9 min. The column was re-equilibrated with 5% B for 14 min before the next run. For online LC-MS/MS analyses, a New Objective (Woburn, MA) Pico Tip (i.d. 8  $\mu$ m) was used for electrospraying with the voltage set at 2 kV. The MS/MS fragmentation spectrum of cross-linked peptides was analyzed using the MS2Assign Automatic Structure Assignment Program (ASAP)<sup>23</sup> and verified manually.

### Cosedimentation Assays.

BPM-F-actin was cross-linked in the presence of cofilin at a 1:1 mole ratio to actin. ANP-cross-linked F-actin, Cys374-Asp11-cross-linked F-actin, and un-cross-linked F-actin were also mixed with equimolar amounts of cofilin. These complexes were incubated with various concentrations of KCl for 20 min and then pelleted in an OPTIMA-TLX120 ultracentrifuge (Beckman Coulters) at 350000g for 20 min. The pellet and supernatant were separated and run on SDS-PAGE for analysis. ImageJ software was used to quantify the Coomassie-stained bands on the gel.

### Analysis of Binding

Transient kinetic measurements were made at 25 ( $\pm$ 0.1) °C with an Applied Photophysics (Surrey, U.K.) SX.18MV stopped-flow apparatus. The excitation wavelength was set to 390 nm, and the emission was monitored at 90° through a 435 nm long-pass colored glass filter. Time courses of noncontiguous binding were measured by mixing acrylodan-labeled cofilin (1–5  $\mu$ M) with 10  $\mu$ M of actin filaments in F-buffer (pH 7.0). Time courses of cofilin

dissociation were measured by mixing an equilibrated mixture of acrylodan-labeled cofilin and actin filaments (5  $\mu$ M) with 50  $\mu$ M unlabeled cofilin. The indicated concentrations are final concentrations after mixing. Time courses of fluorescence change were fitted to single-exponential expressions by nonlinear least-squares fitting using software provided with the instrument. Standard errors in the fits are reported.

Dissociation rates of cofilin from cross-linked actins were measured with an Alphascan fluorimeter (Photon Technology International). Excitation wavelength was set to 390 nm, and the emission was detected at 505 nm. Conditions were the same as in the control above. Fluorescence changes were fitted to single-exponential expressions using SigmaPlot (Systat Software Inc., San Jose, CA).

## RESULTS

### Actin Cross-Linking by BPM Changes in the Presence of Cofilin

Previous results from Tao et al.<sup>18</sup> showed site-specific photo-cross-linking of F-actin with benzophenone-4-maleimide (BPM). In the presence of BPM, G-actin displays no or only slight intramolecular cross-linking. This is not changed by the binding of cofilin to G-actin (data not shown). In contrast to that, BPM forms mainly intramolecular and some minor intermolecular cross-linkings upon photoactivation in F-actin. The maleimide moiety on BPM reacts efficiently with Cys374 on actin while its benzophenone (BP) moiety photoreacts with amino acids nonselectively but with high yield. We thus can monitor the extent and change in F-actin cross-linking by BPM upon binding of various actin binding proteins.

Skeletal F-actin was labeled with BPM and then combined with an equimolar concentration of yeast cofilin. Upon BP photoactivation, F-actin alone (control) formed mainly intramolecular cross-links. In contrast, similar photoactivation of labeled F-actin in the presence of cofilin produced extensive intermolecular cross-linking and virtually no intramolecular cross-links (Figure 1). A cofilin-induced switch from intramolecular to intermolecular cross-linking in F-actin suggests a modification of elements of the F-actin structure that allows for its extensive cross-linking. Repeating the same experiment with skeletal actin and human cofilin-2 yielded similar results (not shown), indicating that the cofilin-induced cross-linking switch is not cofilin isoform specific.

### Actin filaments Are Formed from BPM-Cross-Linked Dimers

To ensure that the BPM-cross-linked dimers could form normal filaments, we first depolymerized the cross-linked filaments and then purified the dimers via gel filtration. We then polymerized the purified cross-linked dimers in F-buffer. EM images of filaments made from cross-linked dimers and un-cross-linked actin show little difference (Figure 2), except perhaps for the presence of some shorter and more flexible filaments among those made from cross-linked dimers (Figure 2B).

## Mapping of Intermolecular and Intramolecular BPM-Cross-Linking Sites on Actin

An F-actin model depicting the positions of cross-linked amino acids is shown in Figure 3. Because the BP moiety photoreacts nonselectively with amino acids, we used LC-MS/MS to determine the amino acids that are cross-linked in the absence and the presence of cofilin (Figure 4). The maleimide moiety nearly always labels the reactive Cys374 on actin, which allowed us to search for cross-linked fragments that had the peptide fragment, KCF or CF, attached to it. For the intramolecular cross-link, we measured a unique peptide of mass 2639.14 Da that corresponds to fragment Ac-DEDETTALVCDNGSGLVK (residues 1–18, 1906.85 Da, monoisotopic mass) that is BPM (277.07 Da) cross-linked to KCF peptide (396.18 Da) and with cysteine alkylation of the 1–18 peptide (57.02 Da). From the MS/MS spectrum, because product ions up to  $y_7$  from the C-terminus and up to  $b_{10}$  from the N-terminus were detected, we concluded that the cross-linking is to Asp11.

We used a similar method to determine the intermolecular cross-linking sites. We assumed that the CF peptide remained attached; we found a unique peptide of mass 1734.89 Da for fragment HQGVMVGMGQK (residues 40–50, 1170.57 Da) that is BPM (277.07 Da) cross-linked to CF peptide (268.09 Da). The maleimide ring of BPM can open by hydrolysis, increasing the MW by 18 Da. An abundant MS/MS product ion at  $m/z$  675.8 is the 2+-charged ion representing the loss of the CF dipeptide plus the maleimide ring from cleavage between the benzophenone and maleimide rings. Because product ions up to  $b_4$  from the N-terminus and up to  $y_6$  from the C-terminus were detected, we concluded that the cross-linking is to Met44 and a potential cross-linking to Met47 is excluded.

### Actin Cross-Linking Inhibits Cofilin Dissociation by Salt

The cofilin-induced shift from intramolecular to intermolecular cross-linking in F-actin prompted us to test cofilin binding to the cross-linked filaments. Because only small amounts of purified BPM-cross-linked dimers could be recovered, we also compared BPM-cross-linked actin with ANP-cross-linked actin due to their similar sites and extent of cross-linking (Figure 5A). ANP forms an intermolecular cross-link between Cys374 and Gln41 in the DNaseI loop of actin,<sup>19</sup> i.e., the same subdomains that BPM cross-links in the presence of cofilin. In general, cofilin binding to actin is known to decrease with increasing salt concentration of the solvent.<sup>24</sup> Indeed, as the salt concentration is increased, the amount of cofilin in the supernatant, i.e., dissociated from F-actin, increases in all actin samples (Figure 5B). In the presence of 0.75 M KCl, ~80% of cofilin is dissociated from un-cross-linked F-actin and thus found in the supernatant (Figure 5B). In contrast, 0.75 M KCl results in only ~22% dissociation of cofilin from BPM-cross-linked actin and ~35% dissociation from ANP-cross-linked actin, revealing that cofilin remains mostly bound to cross-linked actin even at high salt concentrations.

A recent study by Umeki et al.<sup>25</sup> showed that actin mutation on Asp11 affected cofilin binding, inhibiting it almost completely for the D11Q actin. This result raised questions about the direct or indirect role of Asp11 on actin in cofilin binding and prompted us to test the binding of cofilin to F-actin cross-linked intramolecularly, between Cys374 and Asp11. We show that at various concentrations of salt (Figure 5B) the amount of cofilin dissociated from Cys374-Asp11 cross-linked F-actin is approximately the same as from un-cross-linked



F-actin, revealing that cofilin binding is not impacted by a modification/cross-linking of Asp11.

To shed light on the different effects of salt on cofilin dissociation from cross-linked and un-cross-linked actin (Figure 5B), we measured the rates of cofilin association and dissociation by a stopped-flow method using acrylodan-labeled cofilin. To measure cofilin “on” rates, we used ANP-cross-linked actin, which is prepared in the absence of cofilin,<sup>19</sup> and not BPM-cross-linked actin that is formed in the presence of cofilin. Because of the similar binding of cofilin to ANP- and BPM-cross-linked actin, as measured by sedimentation assays in the presence of salt, we assumed that these two forms of cross-linked actin would behave similarly in binding rate assays. The binding rates for both ANP-cross-linked and un-cross-linked actins were rather similar, with the on rates less than 2-fold lower for ANP-cross-linked actin (Figure 5C). However, a major difference was seen in the dissociation rates. Cofilin dissociation rates from un-cross-linked actin were measured by stopped-flow methods over the course of 10 s, while for both ANP- and BPM-cross-linked actins these measurements were done with a fluorimeter, over the course of minutes. The rates of cofilin dissociation from ANP- and BPM-cross-linked actins (~50% cross-linked) are almost 15 times slower than those from un-cross-linked actin (Figure 5D), suggesting that the reduced flexibility of cross-linked actin impedes cofilin dissociation.

## DISCUSSION

Chemical cross-linking is a valuable tool for probing protein–protein interactions and mapping their possible contact sites. Previous reports have used this technique to map cofilin binding sites to both G- and F-actin.<sup>5,6,8</sup> In combination with MS/MS analysis, we identified in this study the BPM-cross-linked residues in F-actin in the presence and absence of cofilin. Strikingly, the cross-link in F-actin switches from an intra-molecular (Cys374-Asp11) to an intermolecular one (Cys374-Met44) upon cofilin binding.

BPM is a relatively rigid cross-linker. The maleimide moiety of BPM reacts with Cys374 while the BP moiety labels any amino acid within a ~10 Å distance.<sup>26</sup> A recent model of F-actin<sup>27</sup> shows that the distance between residues Cys374 and Asp11 is greater than that between Cys374 and Met44 (Figure 3). Why does then the BP moiety cross-link Asp11 (intramolecularly) instead of Met44 (intermolecularly) to Cys374 in F-actin alone?

Several lines of evidence are consistent with only minor cross-linking of Cys374 to Met44 in F-actin (Figure 1). First, previous attempts to mutate Met44 in yeast actin were unsuccessful, yielding a lethal phenotype and indicating a possible involvement of this residue in actin–actin contacts.<sup>28</sup> Second, a recent model of F-actin structure also supports the involvement of Met44 in important actin–actin contacts,<sup>27</sup> which can shield it from an attack by the BP moiety. Third, the C-terminus of actin is a highly flexible and dynamic region, with the exact position of the attached probe determined mostly by its interactions with the immediate environment. Thus, the fluorescence of Cys374 attached probes changes upon actin polymerization and in some case may even block the polymerization.<sup>29</sup> The empirical evidence of cross-linking Cys374 to Asp11 shows that the distance between the BP moiety on Cys374 and Asp11 must be within ~10 Å, at least transiently.



The binding of cofilin to F-actin blocks the intramolecular (Cys374 to Asp11) cross-linking by BPM and shifts it to an intermolecular cross-linking (Cys374 to Met44). This leads us to consider the structural changes in F-actin that occur upon cofilin binding. Umeki et al.<sup>25</sup> proposed that Asp11 is a critical site on actin for cofilin interaction. In our cosedimentation assays (Figure 5A) there was little difference between the binding of cofilin to Cys374-Asp11-cross-linked F-actin and un-cross-linked F-actin. This suggests that cofilin is not sensing the modification/cross-linking-induced change in Asp11 and therefore, in turn, is unlikely to change the environment or reactivity of this residue. Thus, changes in other sites of actin should be considered to explain the cross-linking shift.

There is ample evidence for structural perturbation of the DNaseI loop in F-actin by cofilin. Muhlrud et al. showed that cofilin binding to F-actin accelerates manyfold the proteolysis of this loop by subtilisin,<sup>30</sup> indicating the loss of the loop's protection and its complete accessibility to the protease. Galkin et al.<sup>4</sup> concluded that the twist change due to cofilin binding causes a substantial displacement of subdomain 2 in actin, resulting in its disordering. The disordering of subdomain 2 leads to a 4-fold increase in F-actin flexibility and disruption of interprotomer contacts,<sup>17</sup> which without cofilin involves probably the Met44 residue. If subdomain 2 is disordered upon cofilin binding, BPM may be able to “capture” the now available Met44, linking it to Cys374. This reaction may be facilitated by the above-mentioned dynamic properties of the C-terminus of actin and the expected effect of cofilin on the orientation/position of the BP probe attached to Cys374. Cofilin-induced changes in the environment of other probes (fluorescent) attached to Cys374 are detected most easily via changes in their fluorescence.<sup>31–33</sup> Our binding data suggest that the dissociation rate of cofilin from actin is greatly reduced by its cross-linking (even at ~50% cross-linking level). The breathing motions of filaments are generally restricted upon cross-linking. It appears that such motions are needed for “unlocking” the bound cofilin even when its affinity for actin is reduced by high ionic strength conditions. It is also feasible that cofilin–actin salt bridges may be re-enhanced by cross-linking, but such a possibility would have to be further tested with mutations.

In conclusion, our study shows the ability to track structural changes in F-actin, both intramolecularly and intermolecularly, through BPM cross-linking. We observe a striking cross-linking shift upon cofilin binding that is consistent with changes observed in the filament twist and dynamics. This method should be useful in studying other F-actin complexes with actin binding proteins to map structural transitions in the filaments at an amino acid resolution. In addition to cofilin, changes in the filament twist have been documented for drebrin<sup>34</sup> and for several actin cross-linking and/or bundling proteins, including scruin<sup>35</sup> and fascin.<sup>36,37</sup> Moreover, changes in the mole ratio of these bundling proteins to actin result in considerable variation in the filament twist change.<sup>35</sup> As documented here for cofilin, it would be attractive to gain more detailed understanding of structural changes in F-actin induced by these proteins.

## Acknowledgments

We thank Dr. Martin Phillips for assistance with using the Applied Photophysics stopped-flow apparatus and Dr. Pinmanee Boontheung for help with the acquisition of the LC-MS/MS data.

## Funding

This work was supported by grants from U.S. Public Health Service grants GM 077190 (to E.R.) and GM 103479 (to J.A.L.). The UCLA Proteomics Center (used for mapping the cross-linked complexes) was established and equipped with a grant from the W.M. Keck Foundation.

## ABBREVIATIONS

<b>BPM</b>	benzophenone-4-maleimide
<b>ANP</b>	<i>N</i> -(4-azido-2-nitrophenyl)putrescine
<b>G-actin</b>	globular or monomeric actin
<b>F-actin</b>	filamentous actin
<b>ADF</b>	actin-depolymerization factor
<b>DNaseI</b>	deoxyribonuclease I
<b>LC-MS/MS</b>	liquid chromatography–tandem mass spectrometry
<b>EM</b>	electron microscopy
<b>SDS-PAGE</b>	sodium dodecyl sulfate–polyacrylamide gel electrophoresis
<b>DTT</b>	dithiothreitol

## REFERENCES

1. Bamburg JR. Proteins of the ADF/Cofilin Family: Essential Regulators of Actin Dynamics. *Annu. Rev. Cell Dev. Biol.* 1999; 15:185–230. [PubMed: 10611961]
2. Bamburg JR, McGough A, Ono S. Putting a New Twist on Actin ADF/Cofilins Modulate Actin Dynamics. *Trends Cell Biol.* 1999; 9:364–370. [PubMed: 10461190]
3. Du J, Frieden C. Kinetic Studies of the Effect of Yeast Cofilin on Yeast Actin Polymerization. *Biochemistry.* 1998; 37:13276–13284. [PubMed: 9748335]
4. Galkin VE, Orlova A, Kudryashov DS, Solodukhin A, Reisler E, Schroder GF, Egelman EH. Remodeling of Actin Filaments by ADF/Cofilin Proteins. *Proc. Natl. Acad. Sci. U. S. A.* 2011; 108:20568–20572. [PubMed: 22158895]
5. Grintsevich EE, Benchaar SA, Warshaviak D, Boontheung P, Halgand F, Whitelegge JP, Faull KF, Ogorzalek Loo RR, Sept D, Loo JA, Reisler E. Mapping the Cofilin Binding Site on Yeast G-Actin by Chemical Cross-Linking. *J. Mol. Biol.* 2008; 377:395–409. [PubMed: 18258262]
6. Mannherz HG, Ballweber E, Galla M, Villard S, Granier C, Steegborn C, Schmidtman A, Jaquet K, Pope B, Weeds AG. Mapping the ADF/Cofilin Binding Site on Monomeric Actin by Competitive Cross-Linking and Peptide Array: Evidence for a Second Binding Site on Monomeric Actin. *J. Mol. Biol.* 2007; 366:745–755. [PubMed: 17196218]
7. Lappalainen P, Fedorov EV, Fedorov AA, Almo SC, Drubin DG. Essential Functions and Actin-Binding Surfaces of Yeast Cofilin Revealed by Systematic Mutagenesis. *EMBO J.* 1997; 16:5520–5530. [PubMed: 9312011]
8. Benchaar SA, Xie Y, Phillips M, Loo RRO, Galkin VE, Orlova A, Thevis M, Muhlrud A, Almo SC, Loo JA, Egelman EH, Reisler E. Mapping the Interaction of Cofilin with Subdomain 2 on Actin. *Biochemistry.* 2007; 46:225–233. [PubMed: 17198393]
9. Pope BJ, Zierler-Gould KM, Kühne R, Weeds AG, Ball LJ. Solution Structure of Human Cofilin Actin Binding, pH Sensitivity, and Relationship to Actin-Depolymerizing Factor. *J. Biol. Chem.* 2004; 279:4840–4848. [PubMed: 14627701]

10. Wriggers W, Tang JX, Azuma T, Marks PW, Janmey PA. Cofilin and Gelsolin Segment-1: Molecular Dynamics Simulation and Biochemical Analysis Predict a Similar Actin Binding Mode. *J. Mol. Biol.* 1998; 282:921–932. [PubMed: 9753544]
11. Dominguez R. Actin-Binding Proteins - A Unifying Hypothesis. *Trends Biochem. Sci.* 2004; 29:572–578. [PubMed: 15501675]
12. Paavilainen VO, Oksanen E, Goldman A, Lappalainen P. Structure of the Actin-Depolymerizing Factor Homology Domain in Complex with Actin. *J. Cell Biol.* 2008; 182:51–59. [PubMed: 18625842]
13. McGough A, Pope B, Chiu W, Weeds A. Cofilin Changes the Twist of F-Actin Implications for Actin Filament Dynamics and Cellular Function. *J. Cell Biol.* 1997; 138:771–781. [PubMed: 9265645]
14. Galkin VE, Orlova A, Lukoyanova N, Wriggers W, Egelman EH. Actin Depolymerizing Factor Stabilizes an Existing State of F-Actin and Can Change the Tilt of F-Actin Subunits. *J. Cell Biol.* 2001; 153:75–86. [PubMed: 11285275]
15. Kudryashov DS, Galkin VE, Orlova A, Phan M, Egelman EH, Reisler E. Cofilin Cross-Bridges Adjacent Actin Protomers and Replaces the Longitudinal F-Actin Interface. *J. Mol. Biol.* 2006; 358:785–797. [PubMed: 16530787]
16. Pfaendtner J, De La Cruz EM, Voth GA. Actin Filament Remodeling by Actin Depolymerization Factor/Cofilin. *Proc. Natl. Acad. Sci. U. S. A.* 2010; 107:7299–7304. [PubMed: 20368459]
17. Galkin VE, Orlova A, VanLoock MS, Shvetsov A, Reisler E, Egelman EH. ADF/Cofilin Use an Intrinsic Mode of F-Actin Instability to Disrupt Actin Filaments. *J. Cell Biol.* 2003; 163:1057–1066. [PubMed: 14657234]
18. Tao T, Lamkin M, Scheiner CJ. The Conformation of the C-Terminal Region of Actin A Site-Specific Photocrosslinking Study Using Benzophenone-4-maleimide. *Arch. Biochem. Biophys.* 1985; 240:627–634. [PubMed: 4026298]
19. Hegyi G, Mák M, Kim E, Elzinga M, Muhrad A, Reisler E. Intrastrand Cross-Linked Actin between Gln-41 and Cys-374. I. Mapping of Sites Cross-Linked in F-Actin by N-(4-azido-2-nitrophenyl)putrescine. *Biochemistry.* 1998; 37:17784–17792. [PubMed: 9922144]
20. Spudich JA, Watt S. The Regulation of Rabbit Skeletal Muscle Contraction. *J. Biol. Chem.* 1971; 246:4866–4871. [PubMed: 4254541]
21. Grintsevich EE, Phillips M, Pavlov D, Phan M, Reisler E, Muhrad A. Antiparallel Dimer and Actin Assembly. *Biochemistry.* 2010; 49:3919–3927. [PubMed: 20361759]
22. Kudryashov DS, Sawaya MR, Adisetiyo H, Norcross T, Hegyi G, Reisler E, Yeates TO. The Crystal Structure of a Cross-Linked Actin Dimer Suggests a Detailed Molecular Interface in F-Actin. *Proc. Natl. Acad. Sci. U. S. A.* 2005; 102:13105–13110. [PubMed: 16141336]
23. Schilling B, Row RH, Gibson BW, Guo X, Young MM. MS2Assign, Automated Assignment and Nomenclature of Tandem Mass Spectra of Chemically Crosslinked Peptides. *J. Am. Soc. Mass Spectrom.* 2003; 14:834–850. [PubMed: 12892908]
24. Cao W, Goodarzi JP, De La Cruz EM. Energetics and Kinetics of Cooperative Cofilin-Actin Filament Interactions. *J. Mol. Biol.* 2006; 361:257–267. [PubMed: 16843490]
25. Umeki N, Nakajima J, Noguchi TQ, Tokuraku K, Nagasaki A, Ito K, Hirose K, Uyeda TQ. Rapid Nucleotide Exchange Renders Asp11 Mutant Actins Resistant to Depolymerizing Activity of Cofilin, Leading to Dominant Toxicity in Vivo. *J. Biol. Chem.* 2013; 288:1739–1749. [PubMed: 23212920]
26. Luo Y, Wu J-L, Li B, Langsetmo K, Gergely J, Tao T. Photocrosslinking of Benzophenone-labeled Single Cysteine Troponin I Mutants to Other Thin Filament Proteins. *J. Mol. Biol.* 2000; 296:899–910. [PubMed: 10677290]
27. Fujii T, Iwane AH, Yanagida T, Namba K. Direct Visualization of Secondary Structures of F-actin by Electron Cryomicroscopy. *Nature.* 2010; 467:724–728. [PubMed: 20844487]
28. Durer ZAO, Diraviyam K, Sept D, Kudryashov DS, Reisler E. F-Actin Structure Destabilization and DNase I Binding Loop Fluctuations. Mutational Cross-Linking and Electron Microscopy Analysis of Loop States and Effects on F-Actin. *J. Mol. Biol.* 2010; 395:544–557. [PubMed: 19900461]

29. Otterbein LR, Graceffa P, Dominguez R. The Crystal Structure of Uncomplexed Actin in the ADP State. *Science*. 2001; 293:708–711. [PubMed: 11474115]
30. Muhlrud A, Kudryashov D, Peyser YM, Bobkov AA, Almo SC, Reisler E. Cofilin Induced Conformational Changes in F-actin Expose Subdomain 2 to Proteolysis. *J. Mol. Biol.* 2004; 342:1559–1567. [PubMed: 15364581]
31. Blanchoin L, Pollard TD. Mechanism of Interaction of Acanthamoeba Actophorin (ADF/cofilin) with Actin Filaments. *J. Biol. Chem.* 1999; 274:15538–15546. [PubMed: 10336448]
32. Carlier MF, Laurent V, Santolini JRM, Melki R, Didry D, Gui-Xian X, Hong Y, Chua NH, Pantaloni D. Actin Depolymerizing Factor (ADF/Cofilin) Enhances the Rate of Filament Turnover: Implication in Actin-Based Motility. *J. Cell Biol.* 1997; 136:1307–1322. [PubMed: 9087445]
33. De La Cruz EM. Cofilin Binding to Muscle and Non-Muscle Actin Filaments: Isoform-Dependent Cooperative Interactions. *J. Mol. Biol.* 2005; 346:557–564. [PubMed: 15670604]
34. Sharma S, Grintsevich EE, Phillips ML, Reisler E, Gimzewski JK. Atomic Force Microscopy Reveals Drebrin Induced Remodeling of F-Actin with Subnanometer Resolution. *Nano Lett.* 2011; 11:825–827. [PubMed: 21175132]
35. Schmid MF, Sherman MB, Matsudaira P, Chiu W. Structure of the Acrosomal Bundle. *Nature*. 2004; 431:104–107. [PubMed: 15343340]
36. Shin H, Grason GM. Structural Reorganization of Parallel Actin Bundles by Crosslinking Proteins: Incommensurate States of Twist. *Phys. Rev. E: Stat., Nonlinear, Soft Matter Phys.* 2010; 82:051919.
37. Claessens MMAE, Semmrich C, Ramos L, Bausch AR. Helical Twist Controls the Thickness of F-Actin Bundles. *Proc. Natl. Acad. Sci. U. S. A.* 2008; 105:8919–8822.

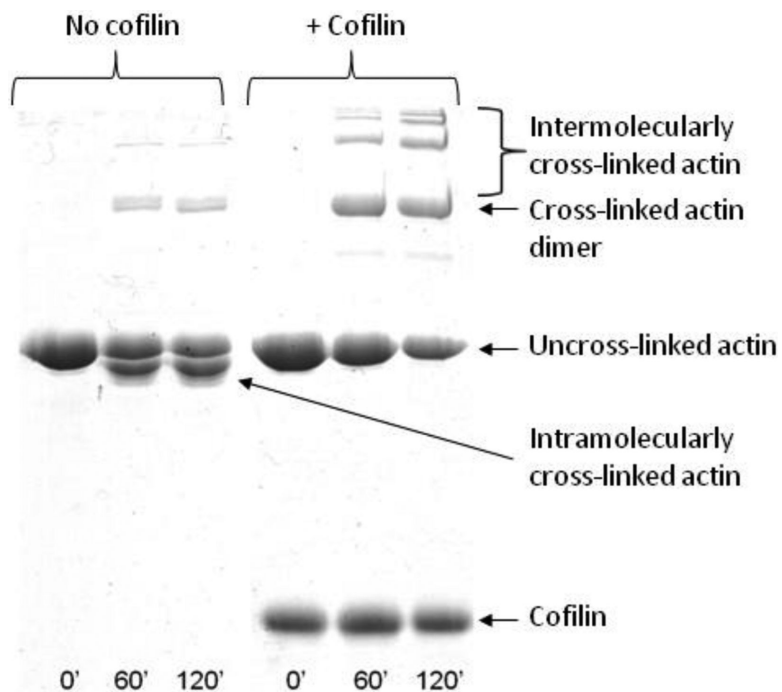


**Figure 1.** Cofilin causes a switch from intramolecular to intermolecular cross-linking by BPM (benzophenone-4-maleimide) in F-actin. Cross-linked products are shown at time points of 0, 60, and 120 min after photoactivation of BPM. Cross-linking reaches a maximum in 120 min. Cofilin migrates at ~16 kDa. Un-cross-linked actin migrates at ~42 kDa. Intermolecularly cross-linked actins migrate at and above ~84 kDa.

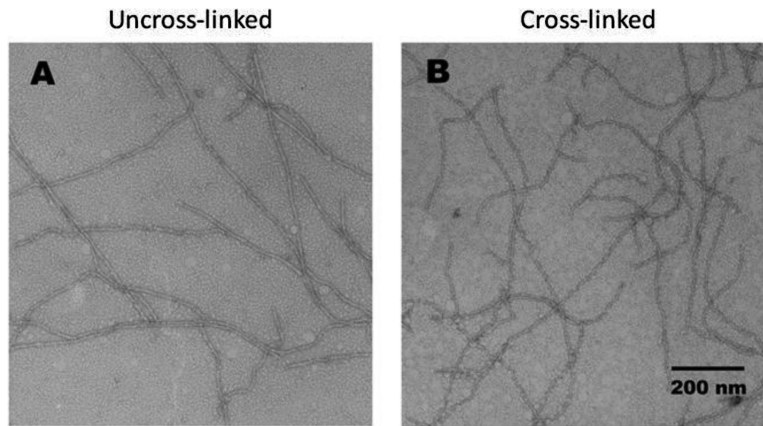


**Figure 2.** EM images of F-actin formed from BPM-cross-linked dimers (B) are similar to those of un-cross-linked actin (A). BPM-cross-linked dimers were purified by gel filtration and then polymerized into F-actin.

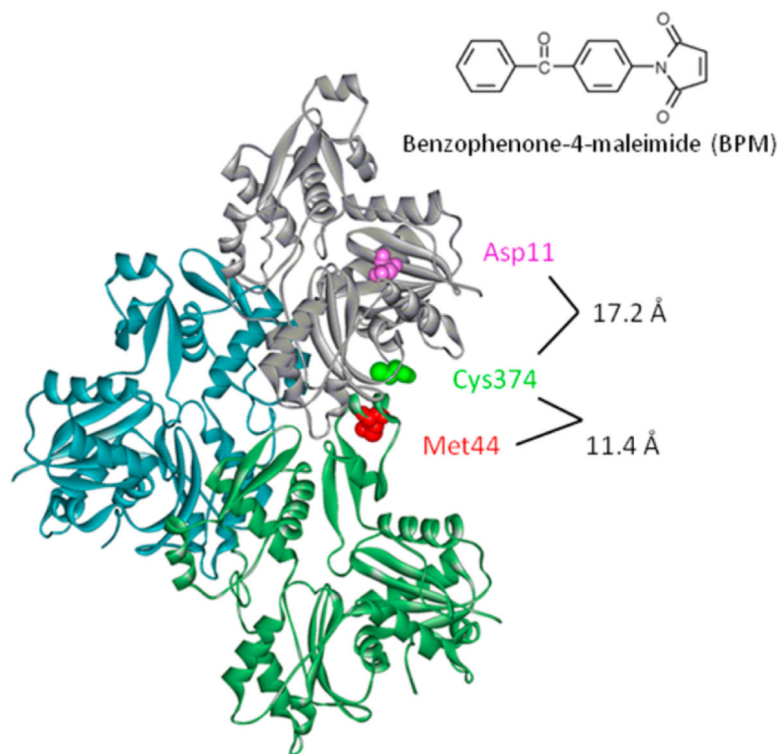


**Figure 3.** Actin sites involved in intermolecular and intramolecular cross-linking by BPM. The amino acids on actin protomers cross-linked by BPM in the presence and absence of cofilin, and the distances between these residues are identified on the model of three actin protomers in F-actin.<sup>27</sup> In the absence of cofilin, BPM cross-links actin intramolecularly between residues Asp11 and Cys 374. In the presence of cofilin, BPM cross-links two actins longitudinally, between residues Met44 and Cys374.



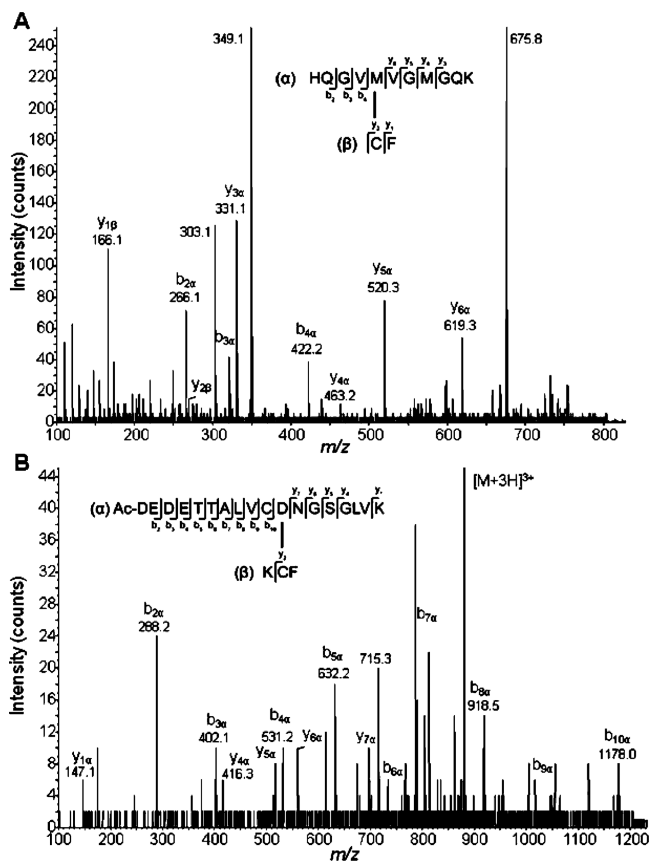


**Figure 4.**

MS sequencing of the BPM-cross-linked actin peptides. (A) MS/MS spectrum of the  $[M + 3H]^{3+}$  of the BPM-cross-linked tryptic peptides at  $m/z$  578.9 in the presence of cofilin. Peptides ( $\alpha$ ) and ( $\beta$ ) are from the same G-actin. Singly and doubly charged  $y$ -type product ions were generated from dissociation of the 3+-charged precursor ion. (Peptide fragments are denoted following the nomenclature for fragmentation of cross-linked oligopeptides. Subscripts are used to denote the residue position, counting from the N terminus for  $a_n$ ,  $b_n$ , and  $c_n$  ions and from the C terminus for  $x_n$ ,  $y_n$ , and  $z_n$  products.) (B) MS/MS spectrum of the  $[M + 3H]^{3+}$  of the BPM-cross-linked tryptic peptides at  $m/z$  880.4 in the absence of cofilin. The representation is the same as in (A).

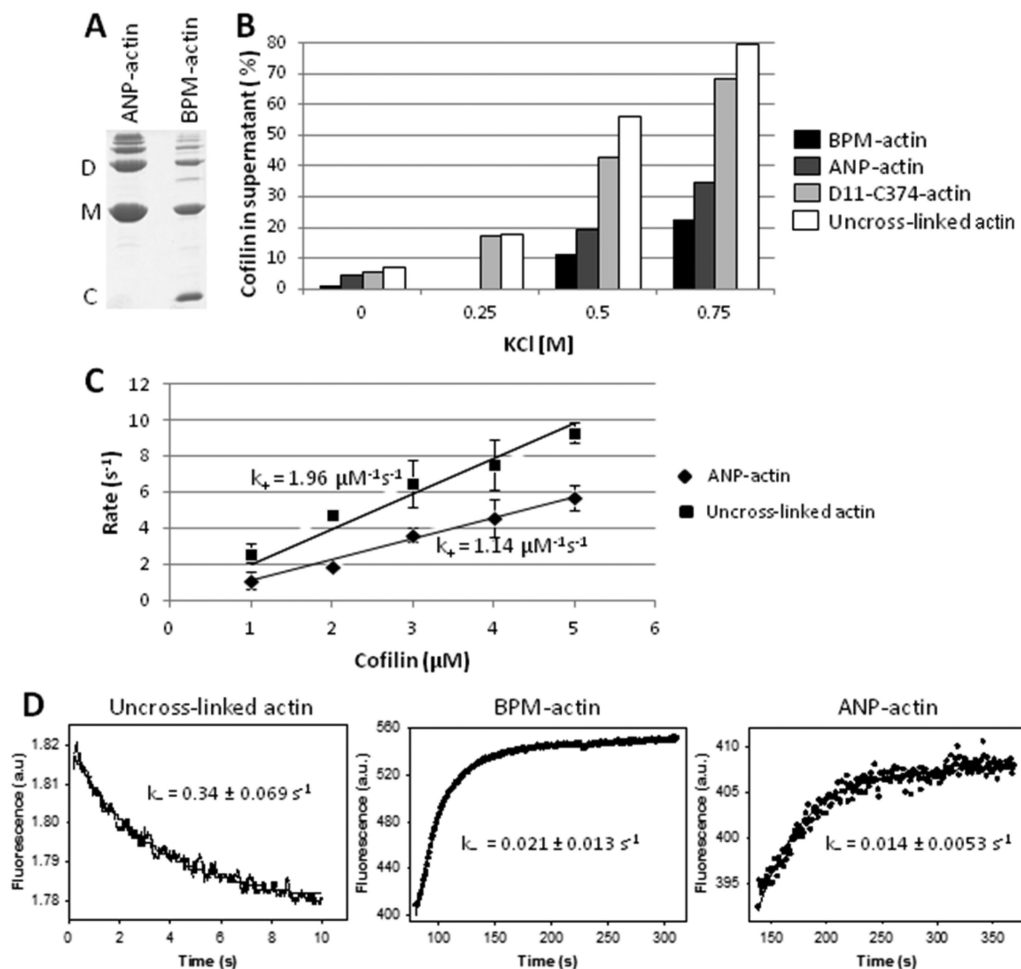


**Figure 5.** Cofilin remains mainly associated with cross-linked actin at high salt concentrations. (A) SDS-PAGE shows the ANP-cross-linked and BPM-cross-linked actin with similar extents of cross-linking. M, D, and C refer to actin monomers, actin dimers, and cofilin. Bands above D on the gel represent higher actin oligomers. (B) The bar graph shows the percentage of cofilin remaining in the supernatant after cosedimentation with F-actin in the presence of increasing amounts of salt. Approximately 20% of cofilin is bound to and cosediments with control F-actin and/or the D11-C374 cross-linked actin in the presence of 0.75 M KCl. In both ANP- and BPM-cross-linked actins, more than 60% of the cofilin remains bound to actin in the presence of 0.75 M KCl. The assay was not performed for ANP- and BPM-actin at 0.25 M KCl because of their relatively small binding changes with the increments of salt. (C) Cofilin binds to un-cross-linked actin (■) at the faster observed rate than to ANP-cross-linked (◆) actin. (D) Rates of cofilin dissociation from un-cross-linked, BPM-cross-linked, and ANP-cross-linked actins. The rates represent an average from 5 to 10 runs. Representative curves of fluorescence change are shown for the three rate measurements. Cofilin bound to BPM- and ANP-cross-linked actins shows almost 15-fold slower rates of dissociation than from un-cross-linked actin.